Journal of Environmental Chemical Engineering 10 (2022) 106977

Contents lists available at ScienceDirect

Journal of Environmental Chemical Engineering

journal homepage: www.elsevier.com/locate/jece

Continuous adsorption studies of pharmaceuticals in multicomponent mixtures by agroforestry biochar

Antón Puga [a,b], Manuela M. Moreira [b], Marta Pazos [a], Sónia A. Figueiredo [b], M. Ángeles Sanromán [a], Cristina Delerue-Matos [b], Emilio Rosales [a,*]

[a] CINTECX, Universidade de Vigo, Grupo de Bioingeniería y Procesos Sostenibles, Departamento de Ingeniería Química, Campus Lagoas-Marcosende, 36310 Vigo, Spain
[b] REQUIMTE/LAQV, Instituto Superior de Engenharia do Instituto Politécnico do Porto, Rua Dr. António Bernardino de Almeida, 431, 4249–015 Porto, Portugal

ARTICLE INFO

Keywords:
Agroforestry biochars
Fixed-bed column
Venlafaxine
Trazodone
Fluoxetine

ABSTRACT

In this study, the adsorption of a multicomponent mixture of active pharmaceutical compounds, such as Venlafaxine (VLX), Trazodone (TRZ) and Fluoxetine (FLX), was studied in a biochar fixed-bed column. The selection of appropriate biochar (eucalyptus, grapevine cane and holm tree biochar) as an adsorbent was carried out through batch assays. An insight into the adsorption mechanism and its correlation with the chosen biochars was performed, showing that electron donor/acceptor interaction is the main mechanism involved. Equilibrium and kinetic batch adsorption experiments were performed and the results demonstrated that eucalyptus biochar was the most viable option for the removal of the pollutants, individually and combined. Column adsorption experiments were performed and Thomas, Yoon-Nelson and Yan models were adjusted to the breakthrough curves. This multicomponent system exhibited a synergetic behavior for TRZ and an antagonist for VLX and FLX, when compared to the single and multicomponent systems previously evaluated in batch assays. The treatment of real wastewaters, spiked with pollutants, has demonstrated the removal efficiency of multicomponent mixtures. Finally, the adsorbent regeneration by elution in different solutions was also investigated and methanol proved to be the most effective eluent for the column regeneration.

1. Introduction

Nowadays, the amount of pharmaceuticals consumed by the human population and ingested by animals (mainly livestock) has experienced a considerable increase [1]. However, their assimilation by consumers is incomplete and causes the release of these compounds (in their original form or as metabolytes) into the wastewater, reaching the wastewater treatment plants (WWTPs), which are often inefficient in their removal [2]. Consequently, they are diffused into the environment and contaminate water sources or even the soil [3,4].

Pharmaceuticals, including antibiotics, analgesics, beta-blockers, etc., have been detected in wastewater and surface waters, in ranges from ng/L to μg/L [5]. Among them, the occurrence of psychiatrics has increased, mainly in hospitals, but also in urban wastewater, as reported by Kosma et al. [6] in some WWTPs in Greece or by Pivetta et al. [7] in WWTPs in Brazil. As their removal cannot be efficiently achieved in WWTPs, it is necessary to find viable treatment solutions that operate in a continuous mode. Other aspects that must be taken into consideration are their low concentration levels (micro-pollutants) and the fact that they are detected in mixtures showing undesirable synergetic effects and become an even more serious threat to deal with [6].

Adsorption is one of the alternative treatments which has attracted increasing interest as an efficient way of treating micro-pollutants with a wide range of operational designs. The most used adsorbent is activated carbon. Nevertheless, several materials have been reported as alternative adsorbents for the removal of organic compounds, including low-cost materials such as clay minerals [8], biomass wastes [9] or carbonaceous materials [10-12]. The use of some waste materials, raw or modified by pyrolysis producing biochar, would lead to their valorization through their use as an adsorbent. Considering that one waste is used to treat another, the circular-economy principles that try to reuse materials as much as possible and reduce waste are followed. Biochar is a low-cost adsorbent material which can effectively treat micro-pollutants as it is reported in the literature [13,14,12]. One of the main drawbacks in the studies is that they are commonly applied to removing single pollutants and not to eliminate a mixture, which has

* Corresponding author.
E-mail address: emiliorv@uvigo.es (E. Rosales).

https://doi.org/10.1016/j.jece.2021.106977
Received 31 July 2021; Received in revised form 11 November 2021; Accepted 7 December 2021
Available online 9 December 2021

barely been studied in the literature. Moreover, scarce results are published about developing a treatment system operating in a continuous flow system.

This study aims to ascertain the simultaneous removal of three antidepressants, Venlafaxine (VLX), Trazodone (TRZ) and Fluoxetine (FLX) which, due to their frequent use, are found in the rivers and waters of Portugal (VLX 55–484 ng/L; TRZ 2–234 ng/L; FLX 57.5–76 ng/L), the United Kingdom (VLX 21.4–285.1 ng/L; TRZ 0.6–27.5 ng/L; FLX 5.6–66.5 ng/L) or Latin America (VLX 55–120 ng/L; FLX 9.8–100 ng/L), with an environmental persistence and bioaccumulation in aquatic organisms [15,16]. For this, three agroforestry biochars, produced from pruning residues, were screened (namely, the holm tree, grapevine cane and eucalyptus). As FLX adsorption by these biochars had been evaluated in a previous investigation [17], in this research an in-depth, individual adsorption study of the other two pollutants (VLX and TRZ) was requested, evaluating their behavior through adsorption kinetics and equilibrium studies. After this, batch tests were conducted on multicomponent mixtures of these pharmaceuticals and compared with the monocomponent studies. Finally, the adsorption process' efficiency for the mixture was investigated through a biochar packed bead column operating in a continuous flow system, using two different water matrices: ultrapure water and real wastewater.

2. Materials and methods

2.1. Chemical reagents

VLX (>99% purity), TRZ (≥99% purity) and FLX (>98% purity, Table SM1) were purchased from Sigma-Aldrich. Formic acid (99% purity) and acetonitrile, both HPLC grade for mobile phases, were purchased from VWR Chemical BDH Prolabo. Diluted solutions of hydrochloric acid and sodium hydroxide (purity > 99%), supplied by VWR, were used for pH adjustments.

Milli-Q grade water was used as a solvent in all the solutions, except in assays that used wastewater from the outlet of a WWTP situated in the north of Portugal.

2.2. Biochar preparation and characterization

The biochars from pruning residues of grapevine cane biochar (GB), holm tree biochar (HB), and eucalyptus biochar (EB) were prepared, as previously described by Fernandes et al. [17]. Briefly, the procedure was as follows: oven heating to 500ºC for 8 h, which was maintained for 14 h and finally cooled down to room temperature for 18 h. Each biochar was prepared by pyrolysis without gas supply and only with the oxygen from the biomass. Prior to use, the biochars were ground and sieved to give a regular particle size (<75 μm).

The biochars were characterized and their moisture, ash and volatile matter composition were determined, as described by Fernandes et al. [17]. The atomic ratios (O/C and H/C) were calculated based on elemental analysis.

The surface morphology of the biochars was studied using Scanning Electron Microscopy (SEM) and Energy Dispersive Spectrometry (EDS). SEM was performed on a JEOL JSM-6700 F SEM equipped with an EDS Oxford Inca Energy 300. The specific surface area (BET) and pore size distribution were determined by the single point Brunauer, Emmett and Teller (BET) method using a Micromeritics ASAP 2020. The FTIR analysis was performed using a FTIR spectrometer (Nicolet 6700 Thermo) and the functional groups of the biochars were identified by Boehm titration, according to Goertzen et al. [18]. The buffering capacity of the biochars was determined and calculated by the method described by Reddy et al. [19].

2.3. Quantification of pharmaceuticals

The quantification of VLX, FLX and TRZ was performed by high-performance liquid chromatography with a photodiode array and fluorescence detection (HPLC-PDA-FLD), using a Shimadzu LC Prominence system (Shimadzu Corporation, Kyoto, Japan) equipped with a LC-20AB pump, a DGU-20A5 degasser, a SIL-20A autosampler, a SPD-M20A photodiode array detector (PDA) and a RF-10A-XL fluorescence detector (FLD). The control of the chromatographic system and the acquisition and processing of chromatographic data were made using LC solution version 1.25 SP2 software.

Chromatographic separation was carried out using a Luna C18 column (150 ×4.6 mm, 5 μm, Phenomenex, USA) at 35ºC. A gradient program was utilized to separate the pharmaceuticals, operating at a flow of 1 mL/min with 0.1% aqueous formic acid (eluent A) and acetonitrile (eluent B) as mobile phases. The following elution gradient was applied: 90% A to 20% A in 7 min, returning to the initial conditions in 3 min, followed by re-equilibration of the column in 4 min. The injection volume was 20 μL. Fluorescence detection was performed at the excitation/emission wavelength pair of 230 and 290 nm for VLX and FLX, and UV detection for TRZ was performed at 246 nm.

The identification of the pharmaceutical compounds in aqueous solutions was accomplished by comparing the retention times with those obtained for their pure standards and quantification was performed using the external calibration curve method. For that, different concentrations of the mixture of the three components were prepared in water, by dilution of the appropriate amounts of the stock solutions (1000 mg/L prepared in acetonitrile). Relevant analytical data, namely the limit of detection (LOD), limit of quantification (LOQ), and intra and inter-day method precision, are shown in Table SM2. The concentration of each pharmaceutical found in the samples resulted from triplicate injections.

2.4. Preliminary adsorption tests

The biochar adsorption batch studies were performed in 50 mL flasks, with 25 mL of solution of VLX or TRZ (20 mg/L) and 0.25 g of biochar, stirred at 400 rpm (Multistirrer 15, Velp Scientifica) for 120 min at room temperature (20 °C) and natural pH. After that time, an aliquot was collected and centrifuged (14.500 rpm for 10 min at 4 °C) using a Heraeus Fresco 21 Microcentrifuge (Thermo Scientific). Supernatant was analysed by HPLC to determine the concentration of VLX and TRZ.

2.5. Adsorption kinetic studies

In the kinetic batch tests, 250 mL of a monocomponent solution of VLX or TRZ (2 mg/L) was utilized. According to the biochar tested, the amount used was different: 0.125 g for EB and 0.25 g for the others. The assays were kept stirred at 400 rpm (Multistirrer 15, Velp Scientifica) and room temperature (20 °C) for 120 min (VLX) and 180 min (TRZ). The contact time was selected according to the preliminary results obtained with the biochars. To determine the concentration of VLX and TRZ over time, aliquots (1 mL) were collected regularly during the experiment, centrifuged and analysed by HPLC (Section 2.3). All tests were accomplished in duplicate and a blank test was run for each test performed.

Two commonly used kinetic models were selected, Pseudo-first and Pseudo-second order (Eq. 1–2, Table 2), to fit the experimental values.

2.6. Adsorption equilibrium studies

In equilibrium batch tests, 25 mL of a monocomponent solution of VLX or TRZ (2 mg/L) was utilized. The amount of adsorbent used to determine the isotherms varied from 2 to 80 mg. Agitation (Multistirrer 15, Velp Scientifica) was kept at 400 rpm at room temperature (20 °C) for 120 min (VLX) and 180 min (TRZ). Then, 1 mL aliquot was collected, centrifuged, and analysed by HPLC (Section 2.3). All the tests were accomplished in duplicate and a blank test was run for each test

Table 1
Raw materials and biochar characterization values.

		Raw E	EB	Raw H	HB	Raw G	GB
Atomic ratio	O / C	0.69[a]	0.11	0.61[b]	0.13	0.71[c]	0.10
	H / C	1.36[a]	0.22	2.00[b]	0.28	1.71[c]	0.26
	(N + O)/C	0.71[a]	0.12	0.60[b]	0.13	0.73[c]	0.11
Total pore volume (cm^3/g)		–	0.17	–	0.10	–	0.03
Ashes (%)		6.20[a]	1.67	2.90[b]	4.55	6.80[c]	5.90

[a] data obtained from Pereira et al. [20]
[b] data obtained from López-Cano et al. [21]
[c] data obtained from Enes et al. [22]

performed. A similar procedure was followed to evaluate the VLX, TRZ and FLX mixtures.

Three common isotherm models were used, Langmuir, Freundlich and Dubinin-Radushkevich (Eq. 3–5, Table 2), to fit the experimental values.

2.7. Continuous flow studies

The continuous flow test was performed using a glass column (Omnifit) (15 cm height x 2.5 cm diameter) and a peristaltic pump (Gilson, Minipuls 3). The column was filled with 0.4 g of adsorbent and 32 g of silica sand (previously washed). The sand was employed as dispersive material, placed in two layers: 16 g above and 16 g below the biochar. The multicomponent solution containing 2 mg/L of each pollutant (VLX, TRZ and FLX) was pumped at a 4 mL/min flow rate. During the experiment, samples were collected and analysed by HPLC, as described in Section 2.3. Two tests were performed, using different matrices for ultrapure water and real wastewater; both were contaminated with the pharmaceutical mixture.

The Thomas, Yoon-Nelson and Yan models (Eq. 8–10, Table 4), were used to adjust the experimental values.

2.8. Biochar regeneration

The regeneration of the biochar was evaluated by using several desorbing agents (water, water-acetonitrile, acetonitrile and methanol). The spent biochar, previously dried, was submersed in a solution containing the desorbent agent. The solid/liquid ratio was 0.4 g biochar for 150 mL of solution and the contact time was 60 min. After that, the concentration of the pollutants in the liquid was measured by HPLC (Section 2.3).

2.9. Parameter estimation

The experimental data obtained from the kinetic, equilibrium studies were fitted to the described model by nonlinear regression using Sigmaplot (Systat). The goodness of the fitting was observed by the determination of the standard deviations and regression coefficients.

3. Results and discussion

The present study focuses on developing a simple and economical process for treating contaminated water flows by a mixture of FLX, VLX and TRZ. For this purpose, a biochar packed bead column system was

Table 2
Kinetics, equilibrium isotherms and mass transfer model fittings of the monocomponent systems.

Models	Parameters	EB		HB		GB	
		VLX	TRZ	VLX	TRZ	VLX	TRZ
Pseudo-first order $dq/dt = k_1 \cdot (q_e - q_t)$ (1)	q_e(mg/g)	2.60 ± 0.02	3.93 ± 0.01	0.89 ± 0.01	1.58 ± 0.02	0.72 ± 0.01	1.46 ± 0.01
	k_1(1/min)	1.44 ± 0.14	4.89 ± 0.75	2.56 ± 0.40	2.52 ± 0.71	4.40 ± 3.24	3.02 ± 0.39
	R^2	0.9777	0.9994	0.9984	0.9473	0.9741	0.9940
	SEE	0.0952	0.0218	0.0268	0.0880	0.0278	0.0268
Pseudo-second order $dq/dt = k_2 \cdot (q_e - q_t)^2$ (2)	q_e(mg/g)	2.67 ± 0.02	3.95 ± 0.01	0.89 ± 0.01	1.61 ± 0.02	–	1.47 ± 0.01
	k_2(1/min)	1.25 ± 0.14	16.14 ± 4.55	14.29 ± 4.72	2.33 ± 1.34	–	14.68 ± 6.25
	R^2	0.9920	0.9996	0.9857	0.9629	–	0.9938
	SEE	0.0559	0.0174	0.0252	0.0738	–	0.0272
Langmuir $q = q_{max} \cdot b_L \cdot C/(1 + b_L \cdot C)$ (3)	q_{max}(mg/g)	2.79 ± 0.03	8.68 ± 1.39	0.99 ± 0.01	4.56 ± 1.62	0.9 ± 0.36	5.39 ± 0.82
	b_L(L/mg)	33.16 ± 5.26	50.01 ± 17.38	7.94 ± 1.79	2.69 ± 0.83	5.10 ± 0.60	1.39 ± 0.37
	R^2	0.9907	0.9601	0.9585	0.9587	0.9947	0.9588
	SEE	0.1040	0.7107	0.0662	0.2677	0.0423	0.2677
Freundlich $q = K_F C^{1/n_F}$ (4)	K_F ($mg^{1-1/n_F} \cdot L^{1/n_F}/g$)	2.81 ± 0.13	9.48 ± 0.17	0.87 ± 0.01	3.18 ± 0.07	0.62 ± 0.01	3.04 ± 0.41
	n_F	6.25 ± 1.21	5.61 ± 0.42	4.15 ± 0.35	2.76 ± 0.29	4.79 ± 0.42	0.49 ± 0.14
	R^2	0.9460	0.9954	0.9887	0.9872	0.9892	0.9734
	SSE	0.2500	0.2414	0.0346	0.43130	0.0217	0.4313
Dubinin-Radushkevich $q = q_{max} \cdot e^{-\beta\varepsilon^2}$ (5)	q_{max} (mg/g)	4.64 ± 0.06	8.58 ± 0.29	0.94 ± 0.04	3.84 ± 0.30	0.69 ± 0.01	2.14 ± 0.18
	β (mol^2/J^2)	(2.40 ± 0.21)·10^{-9}	(7.00 ± 1.07)·10^{-9}	(2.19 ± 0.41)·10^{-8}	(4.58 ± 1.26)·10^{-8}	(2.64 ± 0.19)·10^{-8}	(2.19 ± 0.36)·10^{-7}
	R^2	0.9698	0.9543	0.8510	0.8150	0.9703	0.9532
	SEE	0.1078	0.0356	0.0769	0.4272	0.0158	0.1391
Linear driving force $t = -\frac{1}{k_p}\left\{\frac{1}{2c}\ln\left[\frac{y_b^2 + a y_b - c}{a - c + 1}\right] + \left(1 + \frac{a}{2c}\right)\left(\frac{1}{\alpha - \beta}\right)\ln\left[\frac{(1-\beta)(y_b - \alpha)}{(1-\alpha)(y_b - \beta)}\right]\right\}$ (6)	k_p (1/min)	3.805	1.135	0.329	0.041	0.145	0.029
	τ_p (min)	0.79	2.64	9.11	71.21	20.72	103.35
	R^2	0.9470	0.9387	0.9099	0.9801	0.931	0.9797
	SEE	7.4668	1.4969	213.2033	7.9030	10.6704	1.0781

Table 3
Parameters for multicomponent adsorption in EB using synthetic and real wastewater.

Models	Parameters	Synthetic wastewater			Real wastewater		
		VLX	FLX	TRZ	VLX	FLX	TRZ
Pseudo-first order	q_e(mg/g)	0.66 ± 0.02	0.77 ± 0.04	0.76 ± 0.05	0.58 ± 0.01	0.76 ± 0.02	0.74 ± 0.06
$dq/dt = k_1 \cdot (q_e - q_t)$	k_1(1/min)	0.16 ± 0.03	4.23 ± 0.65	4.23 ± 0.72	0.10 ± 0.01	0.08 ± 0.01	0.07 ± 0.02
(1)	R^2	0.9700	0.9999	0.9999	0.9991	0.9987	0.9834
	SSE	0.0474	< 0.0001	< 0.0001	0.0098	0.0151	0.0525
Pseudo-second order	q_e(mg/g)	0.71 ± 0.01	–	–	0.65 ± 0.01	0.88 ± 0.06	0.90 ± 0.15
$dq/dt = k_2 \cdot (q_e - q_t)^2$	k_2(1/min)	0.34 ± 0.05	–	–	0.23 ± 0.01	0.13 ± 0.05	0.09 ± 0.07
(2)	R^2	0.9942	–	–	0.9999	0.9942	0.9723
	SEE	0.0209	–	–	0.0033	0.0324	0.0679
Langmuir	q_{max}(mg/g)	1.12 ± 0.02	2.94 ± 0.03	8.82 ± 0.09	1.78 ± 0.01	2.29 ± 0.03	6.48 ± 0.07
$q = q_{max} \cdot b_L \cdot C/(1 + b_L \cdot C)$	b_L(L/mg)	443.23 ± 231.42	24.14 ± 3.46	61.07 ± 5.87	38.35 ± 5.04	52.06 ± 10.03	16.53 ± 3.05
(3)	R^2	0.9226	0.9411	0.9906	0.9963	0.9408	0.9648
	SEE	0.1196	0.2360	0.3460	0.0423	0.1939	0.4432
Freundlich	K_F ($mg^{1-1/n_F} \cdot L^{1/n_F}/g$)	1.08 ± 0.08	2.66 ± 0.11	9.24 ± 0.46	1.73 ± 0.04	2.35 ± 0.05	5.75 ± 0.11
$q = K_F \cdot C^{1/n_F}$	n_F	50.50 ± 28.71	5.33 ± 0.64	4.70 ± 0.53	12.24 ± 2.26	5.55 ± 0.31	4.72 ± 0.31
(4)	R^2	0.8626	0.8838	0.8944	0.9874	0.9828	0.9826
	SEE	0.1593	0.3316	1.1620	0.0777	0.1043	0.3118

Table 4
Parameters of the breakthrough models for CS and CR.

Models	Parameters	Synthetic wastewater			Real wastewater		
		VLX	TRZ	FLX	VLX	TRZ	FLX
Thomas model $\frac{C}{C_o} = \frac{1}{1 + exp\left(\frac{k_{Th}Q_o m}{F} - k_{Th}C_o t\right)}$ (Eq. 8)	Q_0 (mg/g)	1.68 ± 0.11	6.96 ± 0.30	2.36 ± 0.21	1.32 ± 0.11	5.77 ± 0.58	2.31 ± 0.16
	k_{Th} (mL/mg·min)	0.026 ± 0.0	0.003 ± 0.0	0.010 ± 0.0	0.034 ± 0.0	0.005 ± 0.0	0.014 ± 0.0
	R^2	0.9815	0.9434	0.9402	0.9902	0.9859	0.9831
	SSE	0.0542	0.0970	0.0827	0.0420	0.0484	0.0470
Yoon-Nelson model $\frac{C}{C_o} = \frac{exp\left[k_{YN}(t-\tau)\right]}{1 + exp\left[k_{YN}(t-\tau)\right]}$ (Eq. 9)	k_{YN} (1/min)	0.041 ± 0.004	0.009 ± 0.001	0.020 ± 0.002	0.089 ± 0.001	0.013 ± 0.001	0.028 ± 0.002
	τ (min)	64.09 ± 2.26	254.41 ± 2.07	118.92 ± 3.03	50.59 ± 5.13	469.91 ± 32.8	116.63 ± 7.51
	R^2	0.9815	0.9434	0.9402	0.9902	0.9831	0.9859
	SSE	0.0542	0.0827	0.0970	0.0420	0.0484	0.0470
Yan model $\frac{C}{C_o} = 1 - \frac{1}{1 + \left(\frac{F^2 \cdot t}{K_y \cdot q_y \cdot m}\right)^{K_y \cdot C_0/F}}$ (Eq. 10)	k_y (L/min·g)	0.003 ± 0.0	0.002 ± 0.0	0.004 ± 0.0	0.007 ± 0.0	0.004 ± 0.0	0.006 ± 0.0
	q_y (mg/g)	0.71 ± 0.02	3.47 ± 0.10	1.09 ± 0.16	0.27 ± 0.01	2.07 ± 0.12	0.73 ± 0.01
	R^2	0.9965	0.9950	0.9917	0.9893	0.9939	0.9960
	SSE	0.0235	0.0246	0.0360	0.0440	0.0258	0.0281
	Time (min)	VLX	FLX	TRZ	VLX	FLX	TRZ
	τ (C/C_0 0.5)	50.04	108.76	201.80	56.311	85.3264	201.435
	Break point (C/C_0 0.05)	19.35	36.15	53.51	13.08	21.84	38.46
	Saturation point (C/C_0 0.9)	78.03	210.07	406.92	183.21	375.23	658.25

tested for pharmaceuticals removal by adsorption. But before that, it was necessary to know the behavior of each pair of pollutant/biochar in the batch system. To the best of the author's knowledge, only the FLX adsorption on similar biochars has been studied [17]. Therefore, it was necessary to carry out an in-depth adsorption study of VLX and TRZ to individually evaluate their adsorption kinetics and equilibrium behavior.

3.1. Single VLX and TRZ adsorption studies

3.1.1. Preliminary batch adsorption studies with the proposed biochars

Initially, each biochar's ability for the removal of VLX and TRZ, individually, was ascertained (as described in Section 2.4). Concerning TRZ adsorption, the three screened biochars (GB, HB and EB) showed good adsorption with values higher than 90%. In addition, the biochars' adsorption capacities followed the order EB>HB>GB. For VLX, the removal followed the same pattern but with different removal percentages: for HB and GB, elimination values of 72% and 59% were reached, respectively, while complete removal of VLX was achieved when EB was used. The different behaviors observed suggest that different adsorption mechanisms may be involved in the process.

3.1.2. Adsorption mechanisms with the proposed biochars

The adsorption of the selected organic pollutants into the biochars is affected and correlated with the biochar's surface properties (heterogeneity, carbonization degree, etc.), which played a major role in the process [23].

The selected lignocellulosic feedstocks for biochar production are mainly composed of hemicellulose, cellulose and lignin. Their elemental composition (Table 1) involves a high hydrogen/carbon content (H/C ≈ 1.3–2.0) and lower oxygen/carbon content (O/C ≈ 0.6–0.7) with a slight presence of nitrogen and almost no sulfur.

These O/C and H/C ratios could be significantly reduced due to the transformation of organic material into aromatic carbon by thermochemical treatment. Thus, the production of the biochar at the selected operational temperature, 500ºC, causes the thermal degradation of hemicellulose (180–280 ºC), cellulose (240–350 ºC) and lignin (300–500 ºC). This fact is in accordance with Lee et al. [24], who

reported a three-stage biochar production process: pre-pyrolysis (up to 200 ºC), main pyrolysis (200–500 ºC) and formation of carbonaceous products (above 500 ºC), reducing the O/C and H/C ratios. The extent of the process affects the adsorption and it may be linked to non-carbonised biomass with partitioning as a mechanism or, to a greater extent, the reduced ratios influence the adsorption process and suggest adsorption mechanisms, such as electron donor/acceptor interaction, hydrophobic interaction or pore filling.

It is important to know the mechanism involved in the adsorption process, to be able to apply these biochars in the removal of organic pollutants (Fig. 1). In general, the adsorption mechanisms of the pollutants onto biochars may involve pore-filling, hydrophobic interaction, partitioning, electrostatic interaction, π-π or hydrogen bonds [23,25].

3.1.2.1. Electrostatic interaction. One of the most important mechanisms reported in the literature is the electrostatic interaction of adsorbent/adsorbate. Different properties, such as the point of zero charge (pH_{ZPC}), the pKa of the pollutants and solution pH, could explain the favored adsorption of each pollutant onto biochar. In the case of pH_{ZPC}, it provides essential information about the surface charge of the adsorbents and its reliance on the solution's pH. In this sense, the three adsorbents studied, showed pH_{ZPC} values higher than 9.5 (9.75 for EB, 9.61 for GB and 9.59 for HB). At a pH higher than pH_{ZPC}, the biochar tends to be negatively charged while, below the pH_{ZPC}, the surface of the adsorbent tends to be positively charged. It can be observed that the initial pH of both adsorbate solutions containing only TRZ (Fig. 2) or VLX (Fig. 3) are initially below the pH_{ZPC} value, suggesting that the adsorbent's surface charge would be positive. On the other hand, the adsorbate pKa values (Table SM1) are lower than the initial pH, which means that the pollutant speciation is in a positively-charged or neutral form for both pollutants (Figs. 2b and 3b). However, once the biochar is in contact with the solution, the pH dramatically increases for HB and GB after only 1 min of contact time being both basified (Figs. 2a and 3a). This fact is in accordance with Jian et al. [26] who exposed that the high pH of the biochars can be caused by the presence of alkaline inorganic compounds, such as carbonate or silicate, which were not degraded during the pyrolysis, making them alkaline.

Based on the previously exposed, and considering the speciation of

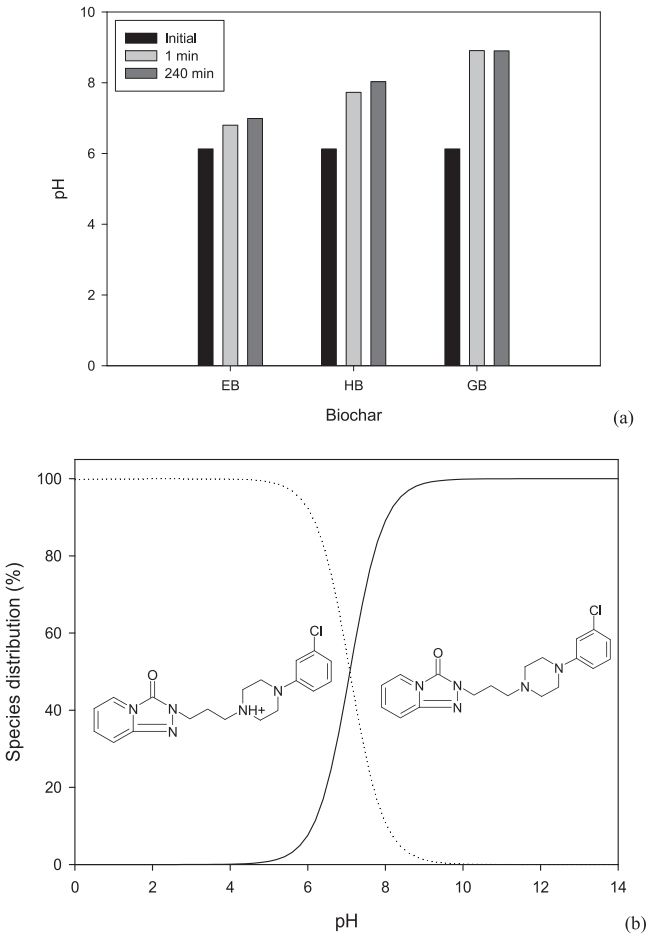

Fig. 2. (a) pH evolution during the single TRZ adsorption assay onto the different biochars; (b) speciation of the pollutant with the pH obtained from Marvin Sketch v. 20.21 (ChemAxom Ltd.).

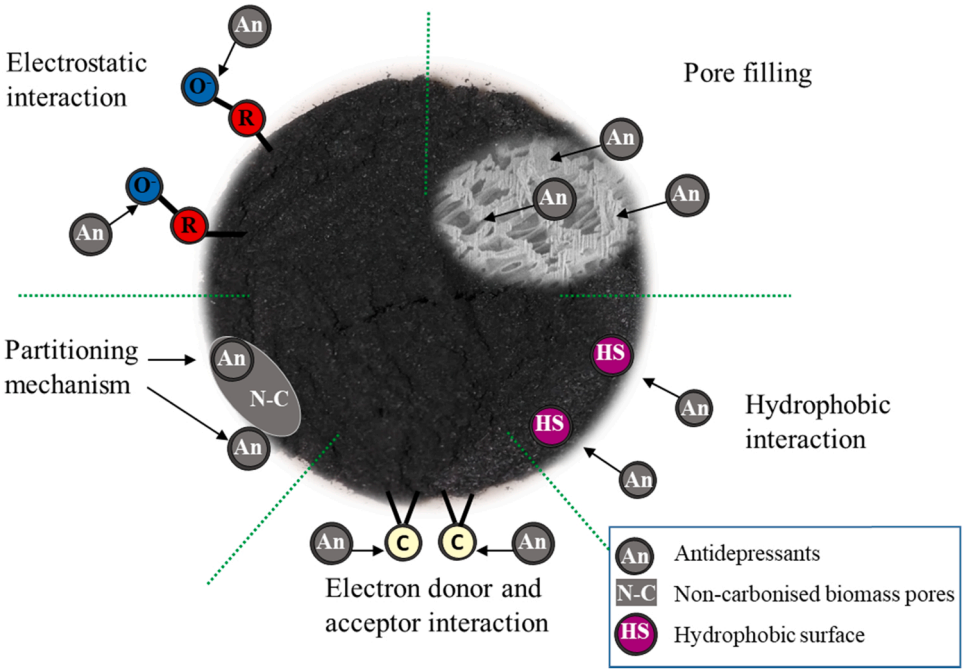

Fig. 1. Pictorial presentation of the mechanisms involved in the adsorption.

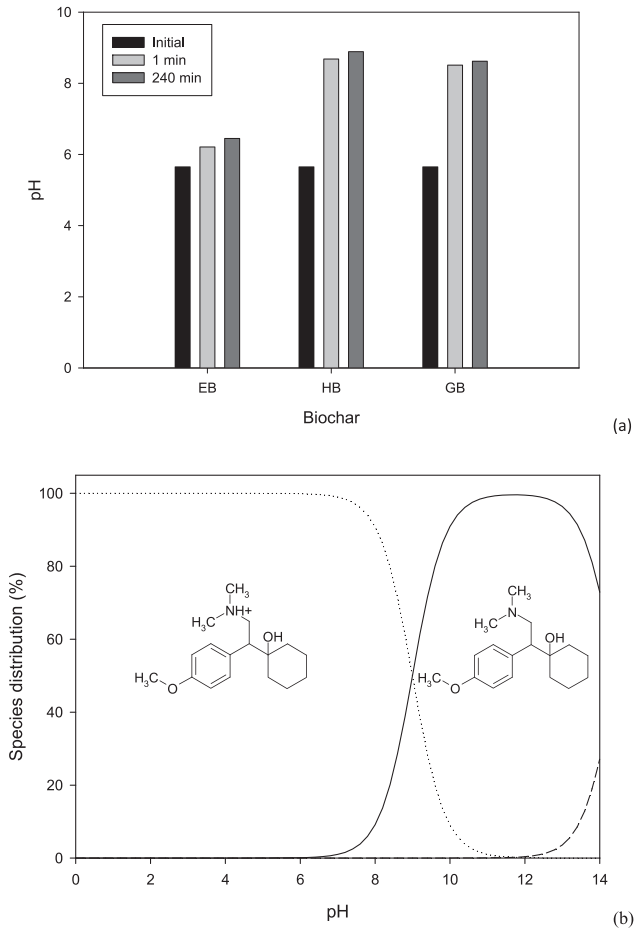

Fig. 3. (a) pH evolution during the single VLX adsorption assay onto the different biochars; (b) speciation of the pollutants with the pH obtained from Marvin Sketch v. 20.21 (ChemAxom Ltd.).

the pollutants displayed in Figs. 2b and 3b, the predominance of positive and neutral species either leads to a repulsion or no interaction among them and the biochar surface. Even though several studies suggest the electrostatic mechanism as being the main, dominant mechanism on the adsorption process for organic pollutants onto biochars [25], other physical or chemical adsorption mechanisms, such as pore filling or π-π interaction, may be key factors in the studied adsorption processes. Therefore, a deeper insight into the biochars' properties by their characterization is required to unveil the process.

3.1.2.2. Partitioning mechanism. The partitioning mechanism is based on the diffusion of the pollutant into the non-carbonised biomass pores. Several authors reported that this mechanism is highly efficient when the biochar has a high volatile matter content [25]. The proximate analysis of the biochars (volatile matter, ashes and fixed carbon content) provides a basic characterization of the prepared biochars (Figure SM1). The low ashes content of the produced biochars (below 5.9%) indicates good combustion in the production process, as well as a similar extent of thermal degradation of the mineral phase in all of them [27]. Besides this, a reduction in the volatile matter content (VM) is observed (e.g., from 79.6% to less than 20.0% in HB), which is related to the pyrolysis of the organic materials present in the raw materials (Figure SM1). According to Mitchual et al. [28], those gases are produced when the biomass is heated in the temperature range 400–500 °C. This process was less efficient for EB (with a VM value of 7.76%), which was at least 2 times less than that measured for GB (16.90%) and HB (18.20%). These results suggest that partitioning could be one of the adsorption mechanisms involved for GB and HB, with a slight influence in EB. The high carbonization degree and prominent carbon content in the selected biochars are evidenced by the fixed carbon content, with values between 70% and 80% [29], reducing the amount of the non-carbonised biochar fraction available for this adsorption mechanism.

3.1.2.3. Electron donor/acceptor interaction mechanism. The different ratios between O, C, H and/or N provide considerable information about the generated biochar properties and also the carbonization degree. The transformation of the organic material to aromatic carbon produced a significant reduction of these O/C and H/C ratios, as displayed in Table 1. The van Krevelen diagram correlates the atomic H/C and O/C ratios with the different carbonization rates of fuels by pyrolization and these ratios decrease with the growing degree of carbonization and increase for low carbonization-degree fuels, such as peat or lignite [30]. Following this diagram, the three biochars' characteristics are related to anthracite and are all classified as Class 1, with higher than 60% carbon content, according to the International Biochar initiative. The H/C ratio is an index that reflects the degree of carbonization; a higher presence of H describes a more disordered biochar C structure [27]. The measured H/C ratios were 0.22, 0.26 and 0.28 for EB, GB and HB, respectively, which are slightly superior to those reported by several authors (H/C ratio <0.2) as suitable for defining black carbon [31]. This means that the produced biochars are not black carbons, presenting similar ratios to those reported for activated carbon [32]. These properties make the selected biochars potential candidates for the electron donor/acceptor interaction mechanism, that is most applied to the adsorption of aromatic compounds on biochar, presenting a graphene-like structure [25].

3.1.2.4. Hydrophobic interaction. This adsorption mechanism is involved when ionizable, organic pollutants are in solution [25]. The O/C ratio is an indicative factor of the hydrophilicity/hydrophobicity of the generated biochars and is related to the presence of polar groups [33]. Low O content resulted in increased hydrophobicity. In these produced biochars, the O/C ratio is quite similar, presenting low values, and this fact, coupled with a low (N + O)/C ratio and polarity index, indicates a scarce presence of oxygenated surface groups [34]. This can favor hydrophobic interaction as a mechanism for the adsorption of hydrophobic and neutral pollutants. Another measure of the hydrophilicity/hydrophobicity of pollutants is the octanol–water partition coefficient (K_{OW}) (Table SM1). TRZ has the highest value for the selected pharmaceuticals (almost 50 times greater), followed by FLX and VLX. The significant difference between the pollutants suggests that the hydrophobic interaction mechanism could explain the good adsorption levels attained for TRZ onto the biochar surface, that also shows hydrophobic properties. This is also in agreement with the reported topological polar surface area values that follow the order: TRZ>FLX>VLX. This could indicate that, in the case of TRZ, more than one mechanism is governing the adsorption.

3.1.2.5. Pore filling. Pore filling is another mechanism involved in the adsorption process. This requires the presence of mesopores and micropores and a small amount of VM. The biochar particle size determination showed that all the produced biochars showed an increase in their particle size distribution from 53.96 μm in EB and 59.53 μm in HB to 72.63 μm in GB and presented a mesoporous structure. The particle size distribution is inversely correlated with the surface area, which decreases in the order: EB (335 m^2/g)> HB (207 m^2/g) > GB (62 m^2/g). It is worth noting that the removal of the VLX and its adsorption capacity is directly correlated to these surface areas and, thus it may be related to the physical adsorption on the surface, as reported by several authors [26,35]. However, as was mentioned before, the adsorption of TRZ onto the biochars showed a completely different behavior, achieving removal levels close to 100%, suggesting that the electron donor/acceptor interation is the most important adsorption mechanism for TRZ.

FTIR analysis confirms the plausibility of the aforementioned

adsorption mechanisms. FTIR spectra of the three biochars showed a characteristic band around 3500–3200 cm^{-1} that can be assigned to the O-H stretching, and C-H symmetric and asymmetric stretching bands related to the aliphatic functional groups were observed at 2910 and 2850 cm^{-1}, respectively. Other bands were observed: at 1629 cm^{-1}, which could be associated with C═C stretching vibrations bonds; a slight band at 1560 cm^{-1}, which was related to carboxylate functional groups; and 1107 cm^{-1}, attributed to the asymmetric stretching vibrations of C–O–C groups [36]. The presence of these scarcely oxygenated groups was confirmed by determining the acidic groups contained in the biochars, resulting in quite similar values of 2.48, 2.65 and 2.51 mmol/g for EB, HB and GB, respectively. The presence of the different acidic groups (carboxilics, lactones and phenolic groups) are shown in Figure SM2. Those acidic groups mainly comprise phenolics, which were 2-fold higher than the determined carboxylic groups and those were slightly superior to the amount of lactones.

Based on the evaluation of the studied biochars and their characterization, a combination of adsorption mechanisms were determined as the most probable taking place. The electron donor/acceptor interation is the most important adsorption mechanism for TRZ, coupled with hydrophobic interaction in all of them suggesting a chemical adsorption. VLX adsorption showed a dependence on the selected biochar and the electron donor/acceptor interation is the main mechanism for EB showing chemisorption as the main phenomena. For GB and HB physorption is suggested with pore filling coupled with partitioning as mechanism.

The development of a column treatment system required a more in-depth description of the adsorption process, demanding the evaluation of the isotherm and kinetic models.

3.1.3. *Batch studies of equilibrium and kinetics*

The optimization of the adsorbent capacity, and its further use in column design, requires knowledge of the interactions between solute and adsorbent, which can be achieved by studying the kinetics and the equilibrium adsorption isotherms.

Kinetic models provide valuable information related to the adsorption pathways and complementary information about the adsorption mechanism involved. Figs. 4a and 5a show the adsorption profiles obtained for all the biochars tested and for each individual compound. In all the assays, it can be observed that EB achieved the best results with an uptake that was 3–4-times higher than that attained with the other adsorbents (GB and HB). Furthermore, HB showed a slightly superior adsorption capacity in comparison to GB. The adsorption was demonstrated to be a very fast process, taking place in a short period (less than 5 min) and with equilibrium being reached in 30 min, for all the biochars tested.

The pH profiles for these assays are shown in Figs. 4b and 5b. As can be seen, the initial solution pH changed. Similar changes in the pH for biochar adsorption have been described by Fang et al. [37], who reported the alkaline effect of biochar, causing a pH increase during their studies (from 4.6 to 9.6). These authors also reported a positive relationship between the increase in pH and the biochar ash content, which agrees with the results obtained in this study.

The most commonly used kinetic models (Pseudo-first and Pseudo-second order model) were selected to adjust the experimental results (Table 2). In the kinetic studies developed for each individual pollutant (Figs. 4 and 5), the VLX adsorption onto HB and GB presented a good fit to the pseudo-first order model while the best fit for the EB was obtained by the pseudo-second order model. The uptake capacity values obtained experimentally (Fig. 4a) under these adsorption conditions ($q_{e,exp}$ 2.65 mg/g for EB, 0.88 mg/g for HB and 0.70 mg/g for GB) were close to the equilibrium uptake values (q_e) determined by the respective kinetic models for each biochar (Table 2).

In TRZ kinetic studies, a different kinetic behavior was observed, and the adsorption mechanisms for this pollutant diverge from VLX. The adsorption of this pollutant onto HB fitted reasonably well with the

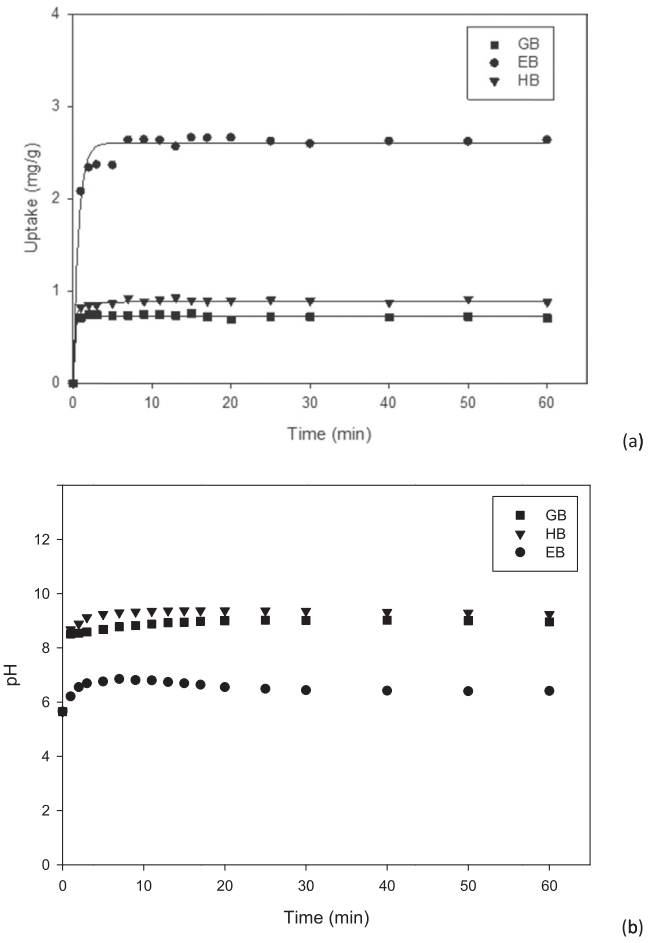

Fig. 4. Adsorption (a) and pH profiles (b) for VLX by different biochars in single-component adsorption tests. (—) Best kinetic model fitting the data.

peudo-second order kinetic model, and the experimental uptake ($q_{e,exp}$ 1.703 mg/g) (Fig. 5a) is slightly inferior to that obtained by the model fitting. On the other hand, EB and GB fit both models well ($R^2 > 0.999$), with a remarkable similarity between the experimental uptake ($q_{e,exp}$ EB 3.96 mg/g and GB 1.46 mg/g) (Fig. 5a) and the values obtained for both models (Table 2). Due to the fact that equilibrium is reached almost immediately, the kinetic results cannot provide more accurate information.

The lack of information about the adsorption mechanism involved in the previous kinetic analysis required a different approach. The mass transfer of the pollutants, from the bulk solution to the adsorbent linking sites, may affect the uptake attained, with several steps being reported in the literature [38,39]. These steps include: (i) the transport of the pollutants in the bulk, which is usually fast; (ii) film transport by diffusion in the boundary layer, which due to the agitation provided can be considered minimal discarding this step as the controlling rate; (iii) the adsorption of the pollutants in the active sites, which overcome the kinetic limitations (according to the results previously reported in this section) and may suggest that this step is the rate-limiting step in the adsorption process. A possible model to evaluate this rate is the Linear Driving Force (LDF) model, represented by Eq. (6) in Table 2 [39]. The results of applying LDF are shown in Table 2 and it can be seen that the particle diffusion coefficient (k_p) decreases in the order EB >HB>GB and with EB coefficient with an order of magnitude 10-times that of, the other biochars.

When the adsorption isotherms were considered, the most commonly used isotherm models (Langmuir, Freundlich and Dubinin-Radushkevich) were selected to evaluate the process (Table 2). The

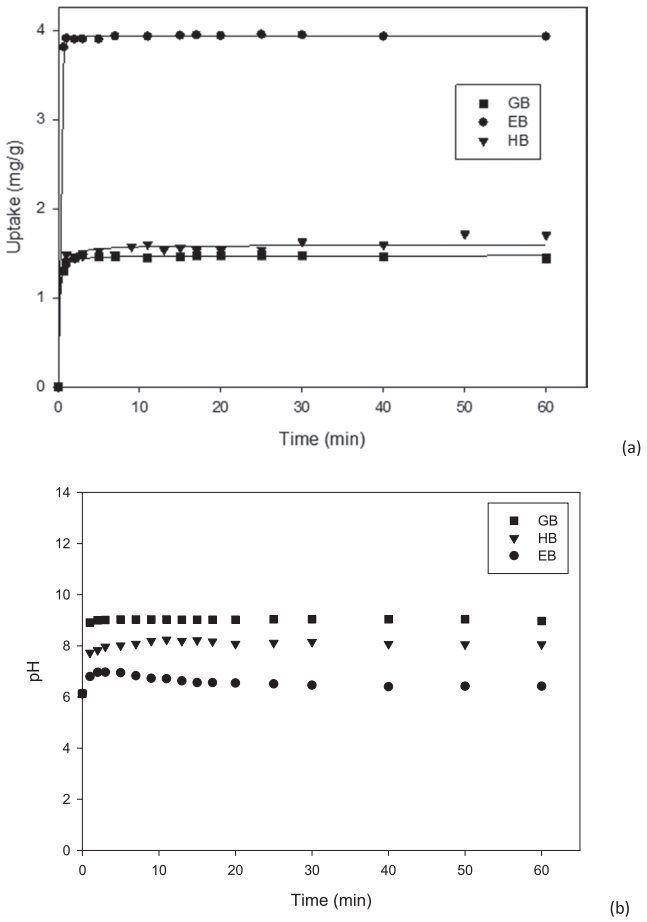

Fig. 5. Adsorption (a) and pH profiles (b) for TRZ by different biochars in single-component adsorption tests. (-) Best kinetic model fitting the data.

maximum adsorption values attained are in the range of the ones reported for VLX in the literature (for vermiculite and marine seaweed) [40]. Concerning TRZ adsorption, there is a lack of information in the literature. The good fitting to the Langmuir isotherm for VLX adsorption onto EB and GB may suggest that the active sites are equally distributed on the surface and the adsorption occurs in a monolayer. Meanwhile, the VLX adsorption on the HB surface presents different behavior, with a better fit to the Freundlich model. This fact suggests that this pollutant's adsorption may occur on a heterogeneous surface [41] and both physisorption or chemisorption can be related to the process. On the other hand, the TRZ adsorption onto the biochar showed the same behavior for all of the biochars, with a better fit to the Freundlich model, suggesting a multilayer adsorption with heterogeneous surfaces. The Dubinin-Radushkevich model allows the distinguishing of the physical or chemical interaction process during the adsorption, determining the mean free energy ($E = 1/\sqrt{2\cdot\beta}$). The adsorption process can be related to chemical adsorption, if this value is between 8 and 16 kJ/mol, and physical adsorption, if the value is lower than 8 kJ/mol [42]. According to the values in Table 2, the mean free energy of EB, HB and GB for VLX was calculated, resulting in 14.400, 1.512 and 1.511 kJ/mol, respectively. The attained value suggests that chemical sorption was the main type of adsorption for EB and also the linking into monomolecular layers, in concordance with the obtained Langmuir fitting. The other two biochars showed physical adsorption for the VLX removal. In TRZ adsorption, the mean free energy for EB, HB and GB was 8.63, 3.30 and 4.35 kJ/mol, respectively, which is similar to that obtained for the other pollutants.

3.2. Multicomponent mixture of pharmaceuticals: batch studies

Once the monocomponent adsorption process was studied (kinetics and equilibrium), the mixture behavior, containing the three psychiatrics, was evaluated and compared with its individual adsorption.

3.2.1. Synthetic wastewater batch studies

The presence of several pollutants on the solution modified the interactions adsorbate/adsorbent previously observed.

The selection of HB and GB as adsorbents led to a substantial decrease in TRZ, FLX and VLX adsorption (~60%), suggesting competitive adsorption among all the species. It can be assumed that the presence of the other two compounds in the mixture reduces the adsorption of VLX and the available active sites on the biochar surface are competitively occupied by FLX and TRZ, leading to the almost null adsorption of the VLX. On the other hand, operating with EB, a competitive adsorptive process was detected between FLX and VLX, resulting in decreased adsorption (of less than 50% of the individual reports). However, the TRZ adsorption was not modified by the other pollutants' presence. This may suggest that the TRZ adsorption mechanism is different from the other components which, apparently, compete by the same linking points. Based on these facts, HB and GB were discarded and the adsorption process analysis was only continued with the most efficient biochar, EB.

A more in-depth insight into EB biochar is required by analysing the fitting data to the classical aforementioned kinetics and equilibrium adsorption isotherms (Table 3).

Kinetic studies showed that the adsorption rate was similar for FLX and TRZ, showing a good fit to the pseudo-first order kinetics with kinetic constants (k_1) of 4.23 and 4.23 1/min, respectively. VLX was a better fit to a pseudo-second order kinetic, as happened in the single adsorption of the pollutant, with a kinetic constant of 0.34 1/min. This behavior, with no precise tailoring to a determinate kinetic model, has been reported in the literature by several authors for FLX in biochar [43] and activated carbons or waste-based biosorbents [44]. Thus, it is not possible to assign a mechanism for the adsorption process (physisorption or chemisorption), based only on the experimental data and fitted kinetic models.

Moreover, considering adsorption isotherms, it can be observed that the best fit was achieved with the Langmuir model. Thus, the theoretical EB maximum uptakes (q_{max}) in the adsorption process of the ternary mixture were compared with the single adsorption, according to the criteria described by Tovar-Gómez et al. [45] and following Eq. (7):

$$R_i = q_{max,i,mixture}/q_{max,i,single};\ i = \text{VLX, FLX or TRZ} \quad (7)$$

The results were: $R_{VLX} = 0.404$, $R_{FLX} = 0.458$, and $R_{TRZ} = 1.017$. According to the literature, a value of $R_i > 1$ indicates that the adsorption process is improved by the presence of the other compounds. Thus, for the TRZ, a synergistic adsorption is happening. However, VLX and FLX showed R_i values lower than 1, meaning that the EB adsorption capacities of these compounds are reduced by a competitive process.

3.2.2. Real wastewater batch studies

The application of the adsorption process and scale up to column requires the study (kinetics and equilibrium) of the treatment process applied to real wastewater (Table 3).

Operating under the same conditions, it is clearly shown that the adsorbed mass of pollutants was different from the observed ultrapure water assays (synthetic wastewater).

The determined adsorption kinetic constants significantly decreased, attaining values of 0.10, 0.08 and 0.07 (1/min) for VLX, FLX and TRZ, respectively, demonstrating that the presence of other compounds in the real wastewater influence the adsorption rate of the adsorbent to the selected pollutants, but allowed the removal of the pollutants at significant levels. This was also confirmed by the isotherm studies. When the

adsorption isotherms are considered, Langmuir fitting showed a decrease in the maximum uptake achieved for FLX and TRZ and a slight increase of VLX adsorption. The co-existence of organic matter, complex pollutants, and ions in the wastewater, significantly influences the adsorption equilibrium as they may exert a competitive or synergetic interaction effect on the process [23].

3.3. Multicomponent mixture of pharmaceuticals: continuous studies

Once the EB's feasibility was demonstrated, the adsorption properties and the effects of the simultaneous pollutant presence were studied, and a complete fixed-bed column adsorption treatment system was proposed.

3.3.1. Synthetic wastewater column study

The system was operated at the same concentration (2 mg/L of each pollutant) until complete saturation was achieved. As depicted in Fig. 6a-c, the saturation time for the column exhibited the following order VLX>FLX>TRZ. This behavior was already expected due to the uptake values attained in the isotherms for the batch assays reported in Section 3.2.2.

The maximum experimental uptake was determined before saturation, resulting in values of 2.07, 2.89 and 7.71 mg/g for VLX, FLX and TRZ, respectively. The comparison of these values with those obtained in the batch assays are presented in Fig. 7a. It can be observed that the adsorbent decreased TRZ uptake (12.67%) and almost kept the same values for FLX (<1%) but, surprisingly, the uptake of VLX was increased in the column assays. This may suggest that the biochar was saturated and the biochar disposition in the column facilitates the contact between VLX and the active points.

Several parameters related to the operation in fixed-bed columns, were calculated and the saturation point τ (time for 50% breakthrough) and breakpoint were estimated (Fig. 7b). The breakpoint of the column was between 19.3 and 53.5 min for VLX, FLX and TRZ. Even though these times could be considered too short for the operation of a column, it needs to be considered that the concentration of the multicomponent mixture is relatively high (at least 10-fold) compared with the values reported in the literature for WWTPs.

The obtained profiles were represented by well-known breakthrough models (Thomas, Yoon-Nelson and Yan models). The plot of the theoretical models and parameters relating to the fitting of the data are presented in Fig. 6 and Table 4. The first model considered was the Thomas model, which assumes a Langmuir equilibrium relationship [46] where the adsorption rate is controlled by the surface reaction between the adsorbate and the unused capacity of the adsorbent. The model's applicability is in consonance with the results obtained in Section 3.2.1 (Langmuir model fitting). As shown in Fig. 6a, this model fitted reasonably well to the VLX breakthrough curve ($R^2 = 0.98$), but it only fits the first section of the breakthrough curve for the adsorption of FLX and is a bad fit for TRZ. The Thomas model has been widely used to determine the maximum adsorption capacity of a column. Fig. 7a displays the maximum uptake values determined by the model and are compared with those attained experimentally in the batch assays. The adsorption capacity estimated by the model parameters was lower than that obtained in the column and batch assays. The badly fit curve can explain this difference. The second model selected was the Yoon-Nelson model, whose expression is mathematically equivalent to the Thomas model [46]. The Yoon-Nelson model is extensively used to determine the rate and breakthrough time of an adsorption column [47]. Like the Thomas model, the same problems in fitting the model to the experimental data were verified (Fig. 6b), presenting the same R^2. The predicted and experimental τ values were different and it was not possible to predict the values from the model (Fig. 7b). It is worth noting that the calculated τ values of VLX, FLX and TRZ were significantly higher than the experimental ones. The last selected model was Yan's model. This model presented a higher correlation coefficient for all the pollutants (R^2 >0.99) and it could precisely predict the experimental data obtained for the three pollutants (Fig. 6c). However, the adsorption capacity (q_y) determined by this model underestimated the uptake capacity by 50%, when compared to the experimental uptake of pollutants adsorbed in the column and the values predicted by the batch assays with the mixture. Similar results, underestimating the model's uptake capacity, have been reported to remove phosphates by lime-iron sludge in column breakthrough studies [48].

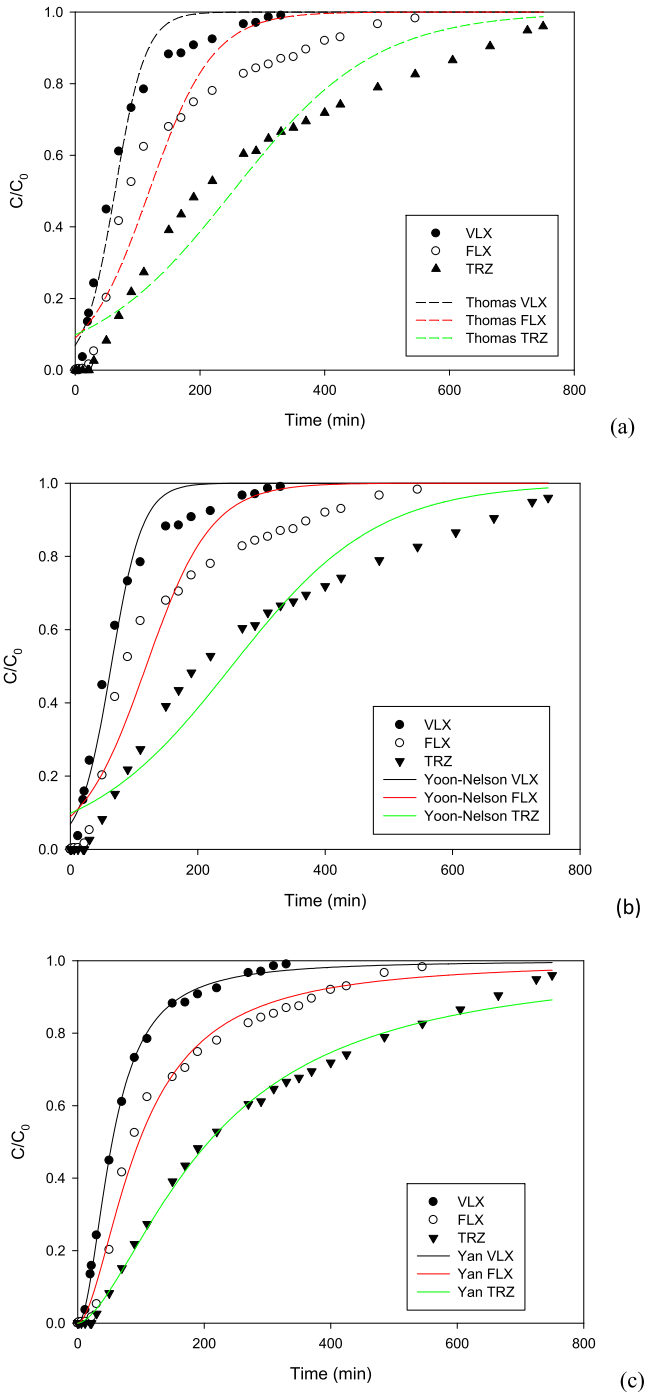

Fig. 6. Breakthrough curves for the adsorption of the pharmaceuticals mixture in spiked synthetic WWTP. The lines represent the fitting to the models: (a) Thomas, (b) Yoon-Nelson and (c) Yan.

3.3.2. Real wastewater column study

The application of the column designed with EB biochar at a bigger

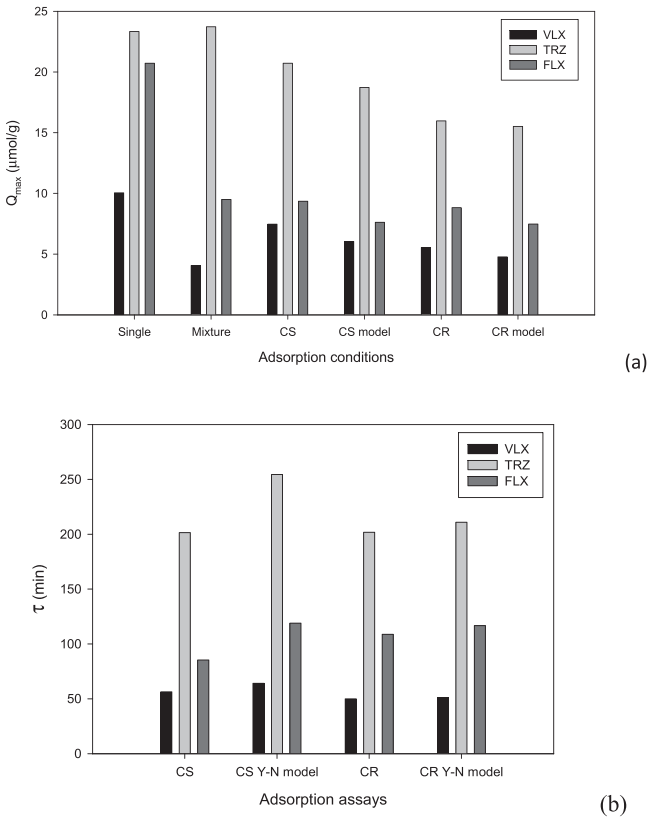

Fig. 7. Results of column assays operating at different conditions: batch single and mixture adsorption, column with synthetic (CS) and real wastewaters (CR) and the respective model parameters concerning the (a) maximum uptake achieved in the removal of each pollutant according to Yan-model and (b) time required for 50% adsorption of each pollutant according to Yoon-Nelson (Y-N).

scale, requires the previous evaluation of its behavior operating with real wastewater. For this purpose, real wastewater, spiked with the three pollutants, was used.

As it includes other compounds, the adsorption process may also be affected by the presence of inorganic or organic compounds that are in the wastewater (e.g. carbonates) and can act as competitive adsorbates (Fig. 8). For this reason, a decrease in the column efficiency can be foreseen. The results confirm this assumption and are in accordance with the previous results attained in the batch assays (Fig. 7 and Table 4). A decrease was observed in the experimental uptake reached in the column, which is quite similar to that obtained in the batch assays. Yoon-Nelson, Thomas and Yan models obtained a good prediction of the VLX, FLX and TRZ adsorption ($R^2 > 0.98$). It is worth noting that the predicted uptake by the Thomas model and the experiments are fairly similar, but they are significantly lower than those attained for the synthetic wastewater. On the other hand, the values obtained by Yoon-Nelson and experimental values for τ were similar for all the considered pollutants. Accordingly, these models can be used in the prediction of the breakthrough curve of the column.

3.4. Regeneration of worn-out adsorbent

The regeneration and reusability of the adsorbent is a key point for the development of an effective, continuous treatment system. A viable desorption method reduces the cost of the treatment and enhances the adsorption-desorption cycles that can be developed in the columns.

Several eluents including water, water-ACN (50%), acetonitrile (ACN) and methanol (MeOH), with polarity indexes between 10.2 and 5.1, were evaluated for the removal of the pollutants mixture (Figure SM3). The biochar regeneration with the more polar solvent and

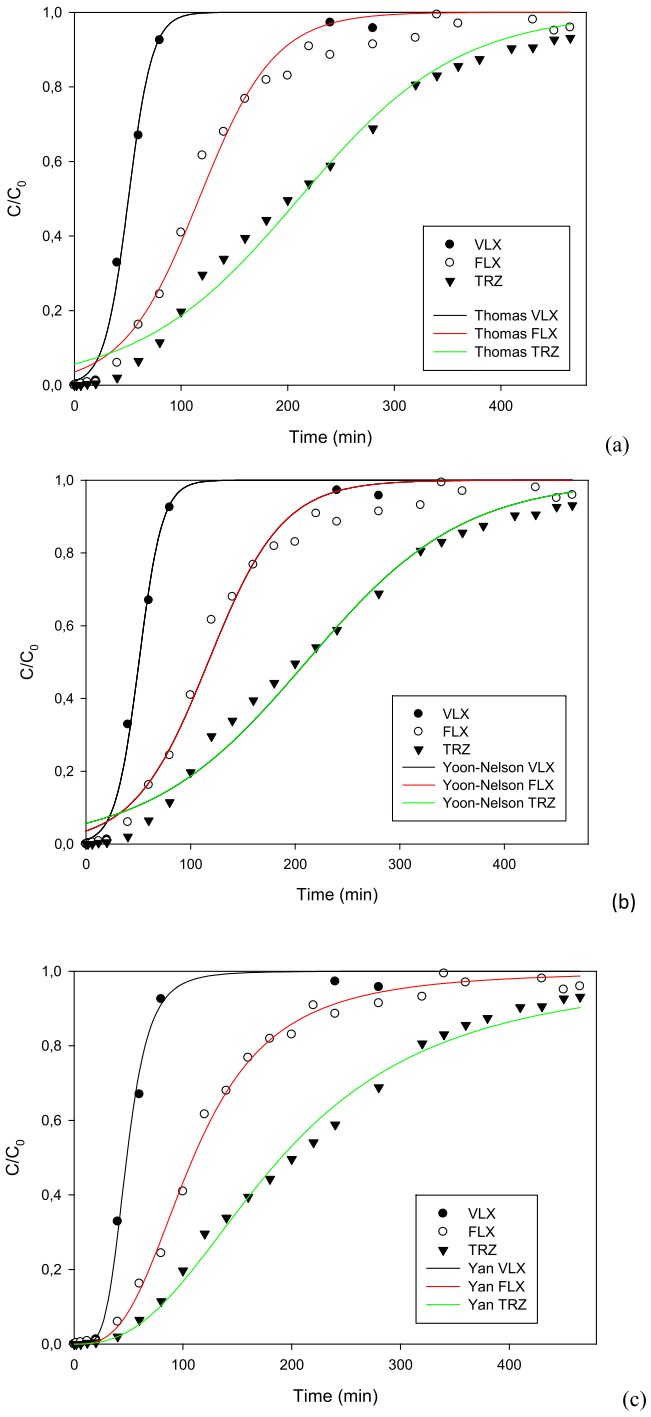

Fig. 8. Breakthrough curves for the adsorption of the pharmaceuticals mixture in spiked real WWTP. The lines represent the fitting to the models: (a) Thomas, (b) Yoon-Nelson and (c) Yan.

water, attained a release of less than 50% of VLX but no effect was noticed in the other two pollutants. This result may be related to the high water solubility value (Table SM1) for the VLX (572 mg/mL) and suggests that part of the adsorption occurred due to physical interactions. When the polarity of the solvent was decreased (water-ACN and ACN), an improvement was observed for FLX and VLX released, with almost total removal of the adsorbed pollutants over a period of 60 min. FLX and VLX were easily displaced compounds by acetonitrile ligand in the adsorbed surface. However, the TRZ was totally adsorbed in the biochar and this may be related to its high octanol-water partition coefficients.

The previous information also confirmed that the adsorption mechanism in the mixture is not the same for all of the pollutants, with VLX and FLX sharing the main mechanism and explaining a competitive adsorption among them. On the other hand, TRZ showed a completely different mechanism. Following the solubility of the pollutants in different solvents (Table SM1), MeOH was selected as the last alternative. Operating with this solvent the pollutant release was total for FLX, VLX and TRZ after 90 min, thus attaining the complete regeneration of the adsorbent. Therefore, the results reinforce the aforementioned difference in the mechanisms for the pollutants in the mixture.

The solvent employed can be evaporated and recuperated for reuse in the desorption process and the pollutants can be treated for degradation by other procedures. Once this operation was performed, the column was operative and could be reused; a two-column system is proposed for further studies.

4. Conclusions

The removal of a multicomponent mixture of pharmaceuticals in synthetic and real wastewaters was successfully carried out in fixed-bed column assays, developed in a continuous mode, simulating a real scenario. The selection of an appropriate adsorbent (EB biochar) facilitates the process of attaining significant removal levels and proves that there are different adsorption mechanisms involved in the adsorption, which are dependent on the selected pollutant properties. This work demonstrates the suitability of the process developed with a biochar from agroforestry waste to solve contamination problems at strategic points, such as hospitals or livestock, or even at the outpoints of WWTPs, reusing the available natural resources.

CRediT authorship contribution statement

Antón Puga: Conceptualization, Investigation, Visualization. **Manuela M. Moreira**: Methodology, Validation, Writing – review & editing. **Sónia A. Figueiredo**: Methodology, Supervision, Writing – review & editing. **Cristina Delerue-Matos**: Resources, Project administration, Funding acquisition. **Marta Pazos**: Data curation, Writing – review & editing. **Emilio Rosales**: Validation, Software, Data curation, Writing – original draft. **M. Ángeles Sanromán**: Conceptualization, Methodology, Supervision, Writing – review & editing, Project administration, Funding acquisition.

Declaration of Competing Interest

The authors declare that they have no known competing financial interests or personal relationships that could have appeared to influence the work reported in this paper.

Acknowlegments

This work has been finantially supported by the project CTM2017-87326-R funded by MCIN/ AEI/10.13039/501100011033/ FEDER "Una manera de hacer Europa", project ED431C 2021/43 funded by Xunta de Galicia and ERDF, and ERA-NET Cofund WaterWorks2015 Call funded by the EU and FCT/UEFISCDE/FORMAS through the REWATER International Research project. This work was also supported by UIDB/50006/2020 and UIDP/50006/2020 by the Fundação para a Ciência e a Tecnologia (FCT Portugal)/Ministério da Ciência, Tecnologia e Ensino Superior (MCTES Portugal) through national funds. Manuela M. Moreira (project CEECIND/02702/2017) also acknowledge for her financial support financed by national funds through FCT and to REQUIMTE/LAQV. Funding for open access charge: Universidade de Vigo/CISUG.

Appendix A. Supporting information

Supplementary data associated with this article can be found in the online version at doi:10.1016/j.jece.2021.106977.

References

[1] T. Lagerberg, Y. Molero, B.M. D'Onofrio, L. Fernández de la Cruz, P. Lichtenstein, D. Mataix-Cols, C. Rück, C. Hellner, Z. Chang, Antidepressant prescription patterns and CNS polypharmacy with antidepressants among children, adolescents, and young adults: a population-based study in Sweden, Eur. Child Adolesc. Psychiatry 28 (2019) 1137–1145, https://doi.org/10.1007/s00787-018-01269-2.

[2] N.A. Alygizakis, P. Gago-Ferrero, V.L. Borova, A. Pavlidou, I. Hatzianestis, N. S. Thomaidis, Occurrence and spatial distribution of 158 pharmaceuticals, drugs of abuse and related metabolites in offshore seawater, Sci. Total Environ. 541 (2016) 1097–1105, https://doi.org/10.1016/j.scitotenv.2015.09.145.

[3] S. Quaik, A. Embrandiri, B. Ravindran, K. Hossain, N.A. Al-Dhabi, M.V. Arasu, S. Ignacimuthu, N. Ismail, Veterinary antibiotics in animal manure and manure laden soil: scenario and challenges in Asian countries, J. King Saud. Univ. - Sci. 32 (2020) 1300–1305, https://doi.org/10.1016/j.jksus.2019.11.015.

[4] R. Wei, F. Ge, L. Zhang, X. Hou, Y. Cao, L. Gong, M. Chen, R. Wang, E. Bao, Occurrence of 13 veterinary drugs in animal manure-amended soils in Eastern China, Chemosphere 144 (2016) 2377–2383, https://doi.org/10.1016/j.chemosphere.2015.10.126.

[5] C.I. Kosma, C.I. Nannou, V.I. Boti, T.A. Albanis, Psychiatrics and selected metabolites in hospital and urban wastewaters: occurrence, removal, mass loading, seasonal influence and risk assessment, Sci. Total Environ. 659 (2019) 1473–1483, https://doi.org/10.1016/j.scitotenv.2018.12.421.

[6] C.I. Kosma, M.G. Kapsi, P.S.G. Konstas, E.P. Trantopoulos, V.I. Boti, I. K. Konstantinou, T.A. Albanis, Assessment of multiclass pharmaceutical active compounds (PhACs) in hospital WWTP influent and effluent samples by UHPLC-Orbitrap MS: temporal variation, removals and environmental risk assessment, Environ. Res. 191 (2020), 110152, https://doi.org/10.1016/j.envres.2020.110152.

[7] R.C. Pivetta, C. Rodrigues-Silva, A.R. Ribeiro, S. Rath, Tracking the occurrence of psychotropic pharmaceuticals in Brazilian wastewater treatment plants and surface water, with assessment of environmental risks, Sci. Total Environ. 727 (2020), 138661, https://doi.org/10.1016/j.scitotenv.2020.138661.

[8] J. Yoshida, K. Tateyama, Y. Kasahara, H. Yuge, Stabilization of oxidized ruthenium complexes by adsorption on clay minerals, Appl. Clay Sci. (2020) 199, https://doi.org/10.1016/j.clay.2020.105869.

[9] A. Silva, W. Stawiński, J. Romacho, L.H.M.L.M. Santos, S.A. Figueiredo, O. M. Freitas, C. Delerue-Matos, Adsorption of fluoxetine and venlafaxine onto the marine seaweed bifurcaria bifurcata, Environ. Eng. Sci. 36 (2019) 573–582, https://doi.org/10.1089/ees.2018.0332.

[10] V. Calisto, C.I.A. Ferreira, J.A.B.P. Oliveira, M. Otero, V.I. Esteves, Adsorptive removal of pharmaceuticals from water by commercial and waste-based carbons, J. Environ. Manag. 152 (2015) 83–90, https://doi.org/10.1016/j.jenvman.2015.01.019.

[11] A. Puga, E. Rosales, M. Pazos, M.A. Sanromán, Prompt removal of antibiotic by adsorption/electro-Fenton degradation using an iron-doped perlite as heterogeneous catalyst, Process Saf. Environ. Prot. 144 (2020) 100–110, https://doi.org/10.1016/j.psep.2020.07.021.

[12] H.N. Tran, F. Tomul, N. Thi Hoang Ha, D.T. Nguyen, E.C. Lima, G.T. Le, C. T. Chang, V. Masindi, S.H. Woo, Innovative spherical biochar for pharmaceutical removal from water: Insight into adsorption mechanism, J. Hazard. Mater. (2020), https://doi.org/10.1016/j.jhazmat.2020.122255 (394).

[13] M.J. Ahmed, P.U. Okoye, E.H. Hummadi, B.H. Hameed, High-performance porous biochar from the pyrolysis of natural and renewable seaweed (Gelidiella acerosa) and its application for the adsorption of methylene blue, Bioresour. Technol. 278 (2019) 159–164, https://doi.org/10.1016/j.biortech.2019.01.054.

[14] J.H.F. de Jesus, T.T. da, G. da, A.S. Mangrich, L.P.C. Romão, Adsorption of aromatic compounds by biochar: influence of the type of tropical biomass precursor, Cellulose (2019) 0, https://doi.org/10.1007/s10570-019-02394-0.

[15] C. Castillo-Zacarías, M.E. Barocio, E. Hidalgo-Vázquez, J.E. Sosa-Hernández, L. Parra-Arroyo, I.Y. López-Pacheco, D. Barceló, H.N.M. Iqbal, R. Parra-Saldívar, Antidepressant drugs as emerging contaminants: occurrence in urban and non-urban waters and analytical methods for their detection, Sci. Total Environ. (2021) 757, https://doi.org/10.1016/j.scitotenv.2020.143722.

[16] P. Paíga, M. Correia, M.J. Fernandes, A. Silva, M. Carvalho, J. Vieira, S. Jorge, J. G. Silva, C. Freire, C. Delerue-Matos, Assessment of 83 pharmaceuticals in WWTP influent and effluent samples by UHPLC-MS/MS: hourly variation, Sci. Total Environ. 648 (2019) 582–600, https://doi.org/10.1016/j.scitotenv.2018.08.129.

[17] M.J. Fernandes, M.M. Moreira, P. Paíga, D. Dias, M. Bernardo, M. Carvalho, N. Lapa, I. Fonseca, S. Morais, S. Figueiredo, C. Delerue-Matos, Evaluation of the adsorption potential of biochars prepared from forest and agri-food wastes for the removal of fluoxetine, Bioresour. Technol. 292 (2019), 121973, https://doi.org/10.1016/j.biortech.2019.121973.

[18] S.L. Goertzen, K.D. Thériault, A.M. Oickle, A.C. Tarasuk, H.A. Andreas, Standardization of the Boehm titration. Part I. CO_2 expulsion and endpoint determination, Carbon 48 (2010) 1252–1261, https://doi.org/10.1016/j.carbon.2009.11.050.

[19] K.R. Reddy, M. Donahue, R.E. Saichek, R. Sasaoka, Preliminary assessment of electrokinetic remediation of soil and sludge contaminated with mixed waste, J. Air Waste Manag. Assoc. 49 (1999) 823–830, https://doi.org/10.1080/10473289.1999.10463849.

[20] B.L.C. Pereira, A.D.C.O. Carneiro, A.M.M.L. Carvalho, J.L. Colodette, A.C. Oliveira, M.P.F. Fontes, Influence of chemical composition of eucalyptus wood on

gravimetric yield and charcoal properties, BioResources 8 (2013) 4574–4592, https://doi.org/10.15376/biores.8.3.4574-4592.
[21] I. López-Cano, M.L. Cayuela, C. Mondini, C.A. Takaya, A.B. Ross, M.A. Sánchez-Monedero, Suitability of different agricultural and urban organic wastes as feedstocks for the production of Biochar-Part 1: physicochemical characterisation, Sustainability (2018), https://doi.org/10.3390/su10072265 (10).
[22] T. Enes, J. Aranha, T. Fonseca, C. Matos, A. Barros, J. Lousada, Residual agroforestry biomass-thermochemical properties, Forests 10 (2019) 1–21, https://doi.org/10.3390/F10121072.
[23] X. Tan, Y. Liu, G. Zeng, X. Wang, X. Hu, Y. Gu, Z. Yang, Application of biochar for the removal of pollutants from aqueous solutions, Chemosphere 125 (2015) 70–85, https://doi.org/10.1016/j.chemosphere.2014.12.058.
[24] X.J. Lee, L.Y. Lee, S. Gan, S. Thangalazhy-Gopakumar, H.K. Ng, Biochar potential evaluation of palm oil wastes through slow pyrolysis: thermochemical characterization and pyrolytic kinetic studies, Bioresour. Technol. 236 (2017) 155–163, https://doi.org/10.1016/j.biortech.2017.03.105.
[25] T.G. Ambaye, M. Vaccari, E.D. van Hullebusch, A. Amrane, S. Rtimi, Mechanisms and adsorption capacities of biochar for the removal of organic and inorganic pollutants from industrial wastewater, Int. J. Environ. Sci. Technol. (2020), https://doi.org/10.1007/s13762-020-03060-w.
[26] X. Jian, X. Zhuang, B. Li, X. Xu, Z. Wei, Y. Song, E. Jiang, Comparison of characterization and adsorption of biochars produced from hydrothermal carbonization and pyrolysis, Environ. Technol. Innov. 10 (2018) 27–35, https://doi.org/10.1016/j.eti.2018.01.004.
[27] D. Aller, S. Bakshi, D.A. Laird, Modified method for proximate analysis of biochars, J. Anal. Appl. Pyrolysis 124 (2017) 335–342, https://doi.org/10.1016/j.jaap.2017.01.012.
[28] S.J. Mitchual, K. Frimpong-Mensah, N.A. Darkwa, Evaluation of fuel properties of six tropical hardwood timber species for briquettes, J. Sustain. Bioenergy Syst. 04 (2014) 1–9, https://doi.org/10.4236/jsbs.2014.41001.
[29] M. Mierzwa-Hersztek, K. Gondek, M. Jewiarz, K. Dziedzic, Assessment of energy parameters of biomass and biochars, leachability of heavy metals and phytotoxicity of their ashes, J. Mater. Cycles Waste Manag. 21 (2019) 786–800, https://doi.org/10.1007/s10163-019-00832-6.
[30] M. Agraniotis, C. Bergins, M. Stein-Cichoszewska, E. Kakaras, High-efficiency pulverized coal power generation using low-rank coals, in: Z. Luo, M. Agraniotis (Eds.), Low-Rank Coals for Power Generation, Fuel and Chemical Production, Woodhead Publishing, 2017, pp. 95–124, https://doi.org/10.1016/B978-0-08-100895-9.00005-X.
[31] T.A.J. Kuhlbusch, P.J. Crutzen, Toward a global estimate of black carbon in residues of vegetation fires representing a sink of atmospheric CO_2 and a source of, Glob. Biogeochem. Cycles 9 (491–501) (1995) O2, https://doi.org/10.1029/95GB02742.
[32] X. Chen, G. Chen, L. Chen, Y. Chen, J. Lehmann, M.B. McBride, A.G. Hay, Adsorption of copper and zinc by biochars produced from pyrolysis of hardwood and corn straw in aqueous solution, Bioresour. Technol. 102 (2011) 8877–8884, https://doi.org/10.1016/j.biortech.2011.06.078.
[33] M. Amin, P. Chetpattananondh, Biochar from extracted marine Chlorella sp. residue for high efficiency adsorption with ultrasonication to remove Cr(VI), Zn(II) and Ni(II), Bioresour. Technol. 289 (2019), https://doi.org/10.1016/j.biortech.2019.121578.
[34] A.W. Samsuri, F. Sadegh-Zadeh, B.J. Seh-Bardan, Characterization of biochars produced from oil palm and rice husks and their adsorption capacities for heavy metals, Int. J. Environ. Sci. Technol. 11 (2014) 967–976, https://doi.org/10.1007/s13762-013-0291-3.
[35] Z. Liu, F.S. Zhang, J. Wu, Characterization and application of chars produced from pinewood pyrolysis and hydrothermal treatment, Fuel 89 (2010) 510–514, https://doi.org/10.1016/j.fuel.2009.08.042.
[36] N. Jamaludin, T.L. Tan, A.S.K. Zaman, A.R. Sadrolhosseini, S.A. Rashid, Empty Fruit Bunch Biochar, Materials 13 (2020), 33556.
[37] Q. Fang, B. Chen, Y. Lin, Y. Guan, Aromatic and hydrophobic surfaces of wood-derived biochar enhance perchlorate adsorption via hydrogen bonding to oxygen-containing organic groups, Environ. Sci. Technol. 48 (2014) 279–288, https://doi.org/10.1021/es403711y.
[38] V.J.P. Vilar, C.M.S. Botelho, R.A.R. Boaventura, Modeling equilibrium and kinetics of metal uptake by algal biomass in continuous stirred and packed bed adsorbers, Adsorption 13 (2007) 587–601, https://doi.org/10.1007/s10450-007-9029-1.
[39] V.J.P. Vilar, C.M.S. Botelho, R.A.R. Boaventura, Equilibrium and kinetic modelling of Cd(II) biosorption by algae Gelidium and agar extraction algal waste, Water Res. 40 (2006) 291–302, https://doi.org/10.1016/j.watres.2005.11.008.
[40] A. Silva, S. Martinho, W. Stawiński, A. Węgrzyn, S. Figueiredo, L.H.M.L.M. Santos, O. Freitas, Application of vermiculite-derived sustainable adsorbents for removal of venlafaxine, Environ. Sci. Pollut. Res. 25 (2018) 17066–17076, https://doi.org/10.1007/s11356-018-1869-6.
[41] D. Li, T. Zheng, Y. Liu, D. Hou, H. He, H. Song, J. Zhang, S. Tian, W. Zhang, L. Wang, J. Ma, A cost-effective Electro-Fenton process with graphite felt electrode aeration for degradation of dimethyl phthalate: enhanced generation of H2O2 and iron recycling that simultaneously regenerates the electrode, Chem. Eng. J. (2020) 394, https://doi.org/10.1016/j.cej.2020.125033.
[42] G. Kirova, Z. Velkova, M. Stoytcheva, V. Gochev, Tetracycline removal from model aqueous solutions by pretreated waste Streptomyces fradiae biomass, Biotechnol. Biotechnol. Equip. 35 (2021) 953–963, https://doi.org/10.1080/13102818.2021.1938677.
[43] S. Escudero-Curiel, U. Penelas, M.Á. Sanromán, M. Pazos, An approach towards zero-waste wastewater technology: fluoxetine adsorption on biochar and removal by the sulfate radical, Chemosphere 268 (2021), 129318, https://doi.org/10.1016/j.chemosphere.2020.129318.
[44] B. Silva, M. Martins, M. Rosca, V. Rocha, A. Lago, I.C. Neves, T. Tavares, Waste-based biosorbents as cost-effective alternatives to commercial adsorbents for the retention of fluoxetine from water, Sep. Purif. Technol. 235 (2020), 116139, https://doi.org/10.1016/j.seppur.2019.116139.
[45] R. Tovar-Gómez, M. Moreno-Virgen, R. del, J. Moreno-Pérez, A. Bonilla-Petriciolet, V. Hernández-Montoya, C.J. Durán-Valle, Analysis of synergistic and antagonistic adsorption of heavy metals and acid blue 25 on activated carbon from ternary systems, Chem. Eng. Res. Des. 93 (2015) 755–772, https://doi.org/10.1016/j.cherd.2014.07.012.
[46] K.H. Chu, Breakthrough curve analysis by simplistic models of fixed bed adsorption: in defense of the century-old Bohart-Adams model, Chem. Eng. J. (2020) 380, https://doi.org/10.1016/j.cej.2019.122513.
[47] S.V. Manjunath, M. Kumar, Simultaneous removal of antibiotic and nutrients via Prosopis juliflora activated carbon column: performance evaluation, effect of operational parameters and breakthrough modeling, Chemosphere (2021), https://doi.org/10.1016/j.chemosphere.2020.127820 (262).
[48] B.S. Chittoo, C. Sutherland, Column breakthrough studies for the removal and recovery of phosphate by lime-iron sludge: modeling and optimization using artificial neural network and adaptive neuro-fuzzy inference system, Chin. J. Chem. Eng. 28 (2020) 1847–1859, https://doi.org/10.1016/j.cjche.2020.02.022.